A&A manuscript no.
(will be inserted by hand later)

Your thesaurus codes are:
06(08.06.2; 08.12.1; 08.16.5; 13.25.5)

ASTRONOMY AND ASTROPHYSICS
9.10.1996

The T Tauri star population in the Lupus star forming region * **

R. Wichmann[1], **J. Krautter**[1], **E. Covino**[2], **J.M. Alcalá**[3,4], **R. Neuhäuser**[3], **and J.H.M.M. Schmitt**[3]

[1] Landessternwarte Königstuhl, D-69117 Heidelberg, Germany
[2] Osservatorio Astronomico di Capodimonte, Napoli, Italy
[3] Max-Planck-Institut für Extraterrestrische Physik, D-85740 Garching, Germany
[4] Instituto Nacional de Astrofísica Optica y Electrónica, A.P. 51 y 216, CP 72000, Puebla, México

Received ; accepted

Abstract. In a recent study, some 130 new *weak-line T Tauri stars* (WTTS) have been discovered in the Lupus star forming region (SFR). Some of these stars are seen projected onto regions of high obscuration, while others are located far from the Lupus dark clouds. In this paper we present photometric observations of a large sample of these WTTS. We estimate effective temperatures and luminosities for the stars observed, and derive masses and ages by comparison with theoretical evolutionary tracks. The mean age of WTTS seen in projection against the dark clouds is found to be lower than the mean age of WTTS discovered far from regions of high obscuration, and yet higher than the mean age of the *classical T Tauri stars* (CTTS) in Lupus. Moreover, while the CTTS in Lupus show an unusual predominance of very low-mass stars, the WTTS population in Lupus contains many stars with comparatively higher masses. Correlations between the X-ray emission and other stellar parameters, like bolometric luminosity, radius, mass, and age, are studied, and the results are discussed.

Key words: Stars: formation – Stars: late-type – Stars: pre-main sequence – X-rays: stars

1. Introduction

Using data from the ROSAT All Sky Survey (RASS), several recent studies (cf. Wichmann et al. 1996, Alcalá et al. 1996a, Sterzik et al. 1995, Neuhäuser et al. 1995b, Krautter et al. 1996) have addressed the problem of the large-scale spatial distribution of pre-main sequence (PMS) stars in star forming regions (SFRs). The exciting result of these studies was that in all the SFRs investigated, the population of X-ray selected weak-line T Tauri stars (WTTS) extends far beyond the regions of high obscuration, where the optically selected T Tauri stars (TTS) - mainly classical T Tauri stars (CTTS) - are located.

As pointed out by Herbig (1978), there should exist a numerous population of TTS that have evolved from the population of CTTS towards the main sequence (post-T Tauri-stars – PTTS) and therefore should show properties already quite similar to those of zero-age main sequence (ZAMS) dwarfs. Only few stars that might belong to this population have been identified so far, since many of the known WTTS are more or less coeval with the CTTS. Since PTTS are by necessity young, they are expected to be active, and hence X-ray surveys provide a powerful tool to search for PTTS candidates.

A comprehensive review of the previous work in Lupus is given by Krautter (1991). Some 69 possible PMS objects have been identified by Schwartz's Hα emission survey (Schwartz 1977). In a recent study Krautter et al. (1996) discovered some 130 new WTTS in the Lupus SFR on the basis of ROSAT X-ray data. We have studied these WTTS photometrically in order to determine their evolutionary status and their relation to the hitherto known population of PMS stars in the Lupus SFR. We are specifically interested in whether these stars represent the long searched-for PTTS or not. We also investigate the history of star formation in the Lupus SFR. Of special interest is the peculiar mass function of the hitherto known Lupus TTS population. We investigate the possibility that the initial mass function in Lupus is time-dependent, i.e. showing a trend towards lower masses with time. Furthermore, we study the relationship between the X-ray and

Send offprint requests to: R. Wichmann

* Based on observations collected at European Southern Observatory, Chile (observing proposals ESO N^o 50.7-0110, 53.7-0085).

** Tables 6 and 7 are only available in electronic form at the CDS via anonymous ftp 130.79.128.5.

non-X-ray characteristics of the Lupus TTS, and discuss the various correlations proposed in the literature.

2. Observations

All photometric observations were performed at the ESO 1 m-Telescope during two observing runs in 1993 and 1994 at ESO, La Silla.

In the first run, three nights (1993 March 10–12) had been allocated for JHKL photometry using the IR Photometer and a nitrogen-cooled InSb detector, and three more nights (1993 March 14–16) for UBVR$_C$I$_C$ photometry with the single channel photometer and a Hamamatsu R 943-02 detector. All nights were photometric.

In the second run, six nights (1994 May 1–6) had been allocated for UBVR$_c$I$_c$ photometry using the single channel photometer and a RCA 31034A detector, and five more nights (1994 May 7–11) for JHKL photometry with the same setup as in 1993. Due to bad weather during the infrared observations, JHKL photometry could only be obtained during two nights (May 10–11), while during the UBVR$_C$I$_C$ observations all nights were photometric.

For the optical (UBVR$_C$I$_C$) photometry a diaphragm of 15 arcsec was used in both runs. The usage of two different instrumental systems (due to a technical problem with the Hamamatsu photo-tube at the second run) does not affect the quality of the photometry, since both systems match very well the Cousins standard system (see Table 2 in Covino at al. 1992). Moreover, each night at least 20 standard stars from the E-regions by Graham (1982) were observed in order to determine the atmospheric extiction coefficients as well as the colour transformation terms for the tie-in to the standard UBV(RI)$_C$ system. Data reduction was performed using the VAX/VMS version of the ESO photometric reduction program SNOPY, using the procedure described in Covino et al. (1992). Typical standard deviations as determined from measurements of standard stars with comparable brightness as the program stars are: $\sigma_V = 0.01$, $\sigma_{B-V} = 0.02$, $\sigma_{U-B} = 0.04$, $\sigma_{V-R_C} = 0.01$, $\sigma_{V-I_C} = 0.01$.

The infrared (JHKL) photometry was measured through a 15 arcsec aperture. For background subtraction standard chopping and beam-switching techniques were applied, using a beam-throw of 20 arcsec in E-W direction. Every night some 12 standard stars from Bouchet et al. (1991) were observed. Data reduction was performed with the IR photometry reduction program available at ESO, La Silla.

Photometric data (with individual errors for the JHKL magnitudes) are given in Table 6.

3. Accretion disks

The presence of optically thick accretion disks can be inferred from the observation of near-infrared excess emission above the photospheric continuum. This excess emission can be measured by

$$\Delta(\mathrm{H}-\mathrm{K}) = (\mathrm{H}-\mathrm{K}) - (\mathrm{H}-\mathrm{K})_0,$$

where (H − K) is the dereddened color of the star and $(\mathrm{H}-\mathrm{K})_0$ the intrinsic color corresponding to its spectral type. Edwards et al. (1993) find $\Delta(\mathrm{H}-\mathrm{K}) \geq 0.09$ for a sample of TTS with spectral types of K7–M1 that show spectroscopic evidence of accretion.

Using the spectral types given by Krautter et al. (1996), we have computed $\Delta(\mathrm{H}-\mathrm{K})$ for all the new TTS of their study for which near-infrared photometry was available, and present the results in Table 7. Only 3 out of 42 stars showed a value of $\Delta(\mathrm{H}-\mathrm{K}) \geq 0.9$. One of them, RXJ 1514.8-4220, is a K1 star which shows Hα in absorption. As this star is quite faint in the infrared, the photometric errors are very large and we doubt that this star really has an optically thick accretion disk.

RXJ1556.1-3655 (= Th 11) shows strong Hα emission (74$\mathring{A}$ equivalent width), thus the presence of an accretion disk is not unexpected. The third star, RXJ1608.6-3922, also shows Hα in emission, with an equivalent width of $\sim 8\mathring{A}$. This value is below the standard limit of $\geq 10\mathring{A}$ for CTTS, but the Hα emission of CTTS is known to be variable, thus this star might well be a CTTS.

However, nearly all of the stars discovered by Krautter et al. (1996) for which infrared photometry is available, do not show any evidence for optically thick accretion disks. This confirms their classification of these stars as WTTS, which was based on the Hα equivalent width alone.

4. Distribution of spectral types

In contrast to other well-studied SFRs like Taurus-Auriga and Chamaeleon, the distribution of stellar masses for the Lupus CTTS is dominated by with very low-mass stars and thus very late spectral types (Krautter 1991, Hughes et al. 1994).

For the study of the distribution of spectral types among the Lupus TTS, as well as for the discussion of other stellar parameters in the following sections, we have divided the data into three subsets, viz. (i) the CTTS, located in regions of high extinction, (ii) the WTTS found in regions of high extinction ('on-cloud' WTTS), and (iii) the WTTS found in regions of low extinction ('off-cloud' WTTS). (We distinguish between regions of high/low extinction qualitatively only, based on the optically visible dark nebulosities as described cf. in Schwartz 1977 and Krautter 1991. Up to now there is no CO survey covering the whole area surveyed by Krautter et al. (1996)).

In Fig. 1 we compare the spectral type distributions for these different subsets of Lupus TTS. It can be seen that the average spectral type of the 'off-cloud' WTTS is much earlier than that one of the TTS known prior to ROSAT, with the 'on-cloud' WTTS exhibiting an intermediate average spectral type. To evaluate the significance

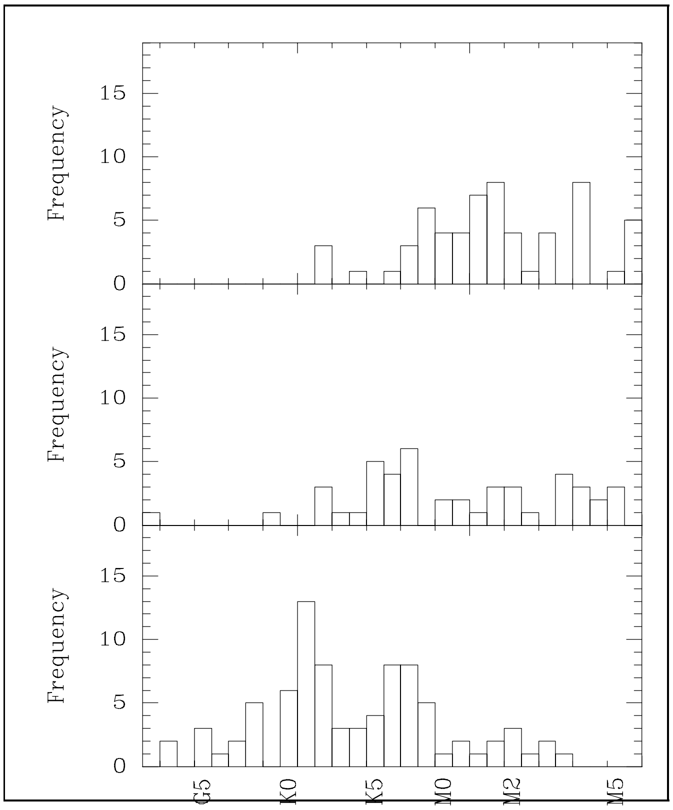

Fig. 1. Distribution of spectral types among the CTTS (upper panel), the 'on-cloud' WTTS (middle panel) and the 'off-cloud' WTTS (lower panel) in Lupus. For the definition of 'on-cloud' and 'off-cloud' WTTS see text.

of the observed differences in the distribution of spectral types, we have performed two-sample Kolmogorov-Smirnov tests. Table 1 shows that the difference in spectral type distribution between the 'off-cloud' WTTS and both the CTTS and the 'on-cloud' WTTS is significant at more than $3\,\sigma$.

Table 1. Results for Kolmogorov-Smirnov tests on the distribution of spectral types. D_{KS} is the maximum discrepancy of both distributions, and P_{KS} the probability for both distributions being drawn from the same parent distribution.

Sample 1	Sample 2	D_{KS}	P_{KS}
$\mathrm{WTTS}_{'\mathrm{off-cloud}'}$	CTTS	0.7076	0.000
$\mathrm{WTTS}_{'\mathrm{on-cloud}'}$	CTTS	0.3944	0.002
$\mathrm{WTTS}_{'\mathrm{off-cloud}'}$	$\mathrm{WTTS}_{'\mathrm{on-cloud}'}$	0.3611	0.002

Stars on the radiative part of the PMS evolutionary tracks evolve towards higher values of T_{eff} (cf. D'Antona & Mazzitelli 1994). Therefore, the observed differences in the distribution of spectral types might indicate a systematic increase in the mean ages from the previously known TTS to the 'off-cloud' WTTS. However, as Neuhäuser et al. (1995a) have shown, there is a correlation between the optical and the X-ray luminosity. As the RASS is flux-limited, the 'off-cloud' WTTS might be biased against stars at the lower end of the mass range.

On the other hand, very young stars are quite luminous and usually very active, with strong optical emission lines, infrared excesses, and powerful outflows, and therefore it seems improbable that previous optical surveys in Lupus have missed such stars (a large fraction of the area of our study has been covered in the objective prism survey by Schwartz (1977). Krautter (1991) and Hughes et al. (1994) have studied the mass distribution of Lupus CTTS and found a significant lack of TTS with masses around $1\,\mathrm{M}_\odot$ or higher in Lupus as compared with other SFRs like, e.g., Taurus-Auriga. We therefore argue that there is a real lack of early-type (i.e. high-mass) stars among the CTTS in Lupus, as compared with the WTTS.

5. Stellar properties

We have estimated the effective temperatures T_{eff} from spectral types given by Krautter et al. (1996), using the calibration of Bessel & Brett (1988) and Schmidt-Kaler (1982).

For the determination of bolometric luminosities $L_\star$ we calculated extinctions towards the individual stars using their (V-I_C) colours and intrinsic colours from Bessel (1991). Then apparent bolometric luminosities were calculated by normalizing a blackbody to the dereddened flux in the R_C band, where the effective temperature of the star was chosen as blackbody temperature. We have checked this method by using the methods described in Alcalá et al. (1996b), i.e. (i) integrating the spectral energy distribution and (ii) using a bolometric correction in I_C. All three methods are found to give consistent results with very small (~ 0.05 dex) systematic differences. Systematic offsets of this size are also found by Alcalá et al. (1996b), see Fig. 1 in their paper. We use the method of blackbody normalization in order to follow the procedure of Hughes et al. (1994), thus enabling us to compare our results directly with their study of Lupus CTTS.

From spectroscopic parallaxes of field stars Hughes et al. (1993) estimated a distance of 140 ± 20 pc for the Lupus SFR. At this distance the angular extent of the area surveyed by Krautter et al. (1996) (about $15^o \times 15^o$ degrees) converts to a linear extent of about 37×37 pc. As WTTS were found not only near the dark clouds, but spread over the whole investigated area, we have to assume that the spatial distribution of WTTS extends radially also a few tens of parsecs from the clouds, thus providing an additional source of error for the bolometric luminosity $L_\star$ of individual stars. However, assuming that the distribution of the stars is more or less uniform in all directions, the

Fig. 2. H-R diagram of Lupus TTS. Filled triangles denote CTTS, filled squares WTTS in regions of high obscuration, open squares WTTS found in regions of low obscuration. Data for CTTS and the WTTS known prior to ROSAT are taken from Hughes et al. (1994). As discussed by Huges et al., the two CTTS below the ZAMS are heavily veiled, thus the extinction may be incorrect.

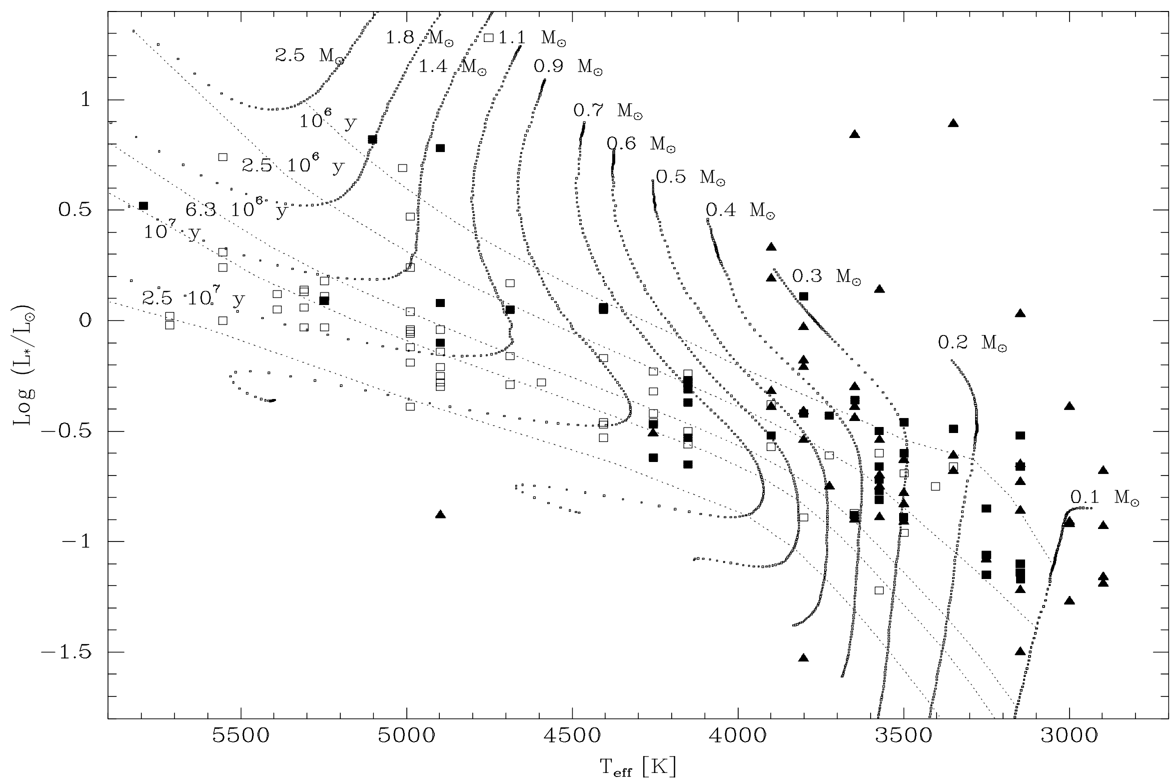

mean distance of the new WTTS in Lupus might not be much different from the mean distance of the CTTS.

Other sources of errors encountered in the determination of T_{eff} and $L_\star$ are thoroughly discussed in Hughes et al. (1994) and Hartigan et al. (1991). Errors in $\log T_{eff}$ are small (± 0.02 dex), but errors in the estimate of A_V can introduce errors in $\log L_\star$ on the order of $\approx \pm 0.1$ dex.

The stellar radii were determined using the effective temperature T_{eff} and the bolometric luminosity $L_\star$. As discussed by Alcalá et al. (1996b), this method yields results in good agreement with the Barnes-Evans method (Barnes & Evans 1976). Based on this consistency, as well as on the study of the scatter in the Barnes-Evans relation by Lacy (1977), we estimate an rms error of about 0.2 dex in $\log R_\star/R_\odot$.

Following Hughes et al. (1994), for the determination of masses and ages we use the evolutionary tracks of D'Antona and Mazzitelli (1994) with Canuto and Mazzitelli convection and Alexander opacities (Alexander et al. 1991). Again, this choice is taken in order to compare our results to the previous study of Hughes et al. (1994). Fig. 2 shows the H-R diagram of the new WTTS in Lupus studied by us. In Table 7 the derived stellar properties are given.

6. Age and mass distribution of Lupus stars

The distributions of ages for our three subsets of Lupus TTS (CTTS, 'on-cloud' WTTS, and 'off-cloud' WTTS) are shown in Fig. 3, and in Table 2 we give mean ages and masses for the three subsets. We performed various statistical tests testing the null hypothesis that CTTS, 'on-cloud' WTTS and 'off-cloud' WTTS have the same age or mass distributions, with the results shown in Table 3. Independently of the statistical test used, this hypothesis can be rejected at a high confidence level for the distribution of the ages as well as for that of the masses of the stars. We conclude that the mean age of the 'off-cloud' WTTS is indeed higher than the mean age of CTTS and 'on-cloud' WTTS.

For undetected binaries the luminosities will be overestimated, and the ages determined from theoretical evolutionary tracks thus will be underestimated. However, while absolut ages might be quite uncertain, conclusions about age differences between Lupus WTTS and Lupus CTTS

Fig. 3. Distribution of stellar ages for CTTS (upper panel), 'on-cloud' WTTS (middle panel), and 'off-cloud' WTTS (lower panel).

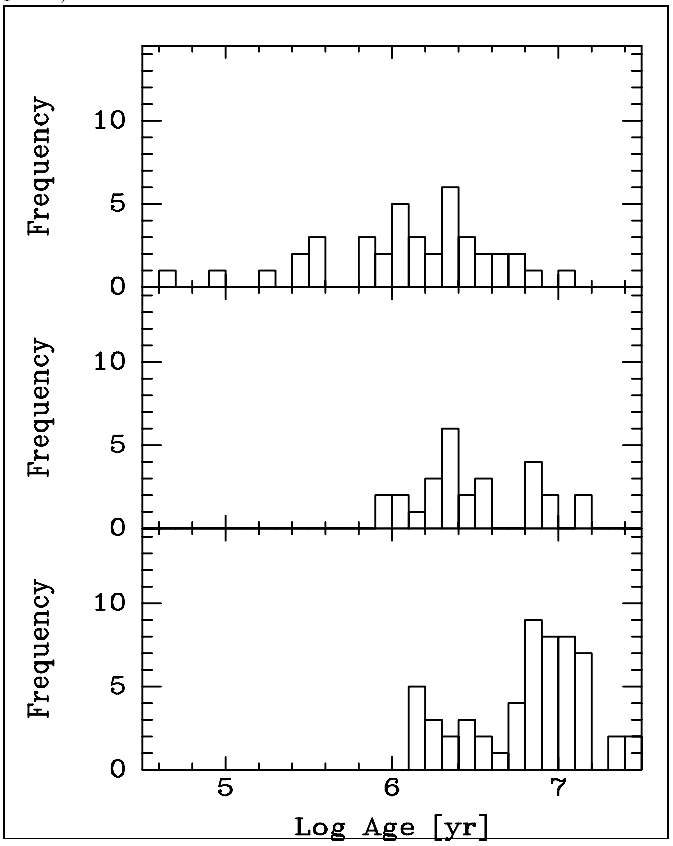

will not be affected much, provided that the multiplicity among both samples is about the same.

Reipurth & Zinnecker (1993) have found 8 binaries in the separation range of 1"–12" in their study of 60 TTS in the Lupus I-III clouds (and for a larger sample extrapolate a high multiplicity fraction of 80-90% for all separations, in line with other studies, cf. Leinert et al. 1993, Ghez et al. 1993, Brandner et al. 1996). The binaries found by Reipurth & Zinnecker (1993) have been taken into account in the study of the optically selected Lupus CTTS by Hughes et al. (1994). Therefore the mean age for this sample might be less underestimated than that of the new WTTS, for which no such binarity study exists. This would even strengthen our conclusion on the 'off-cloud' WTTS being older than the CTTS.

For the discussion of the distribution of masses among Lupus TTS it is important to keep in mind possible selection effects. As already discussed above, there might be a bias against the X-ray discovery of stars with very low masses, but probably not against the optical discovery of high-mass CTTS.

We therefore conclude that the 'present-day' IMF in Lupus, as represented by the youngest TTS in the Lupus SFR, i.e., the CTTS located in the vicinity of the dark

Table 2. Mean ages and masses of Lupus TTS.

Sample	Nr.	Mean log age [yr]	Median log age [yr]
CTTS	45	6.08±0.14	6.15
$WTTS_{'on-cloud'}$	27	6.49±0.07	6.39
$WTTS_{'off-cloud'}$	56	6.81±0.05	6.89
		mass [$M/M_\odot$]	mass [$M/M_\odot$]
CTTS	45	0.31±0.17	0.30
$WTTS_{'on-cloud'}$	27	0.67±0.37	0.69
$WTTS_{'off-cloud'}$	56	0.98±0.36	1.04

cloud cores, shows a significant deficit at higher masses, while obviously in previous periods of star formation in Lupus large numbers of stars with masses of one solar mass or more have been formed. Unfortunately, the bias against X-ray discovery of very low-mass TTS prevents us from estimating the IMF for these earlier periods. In this context, it is very interesting that the Lupus SFR seems to be older than other well-known SFRs like Taurus-Auriga or Chamaeleon (Hughes et al. 1994), which do not show the deficit of high-mass CTTS as observed in Lupus. From our observations, it seems at least possible that the Lupus IMF was similar to the Taurus-Auriga IMF in the past, with the mean mass of newly formed stars shifting towards lower values in later periods.

Table 3. Probabilities P for correctness of the hypotheses of equal distribution of ages and masses among different samples of Lupus TTS. $WTTS_1$ are 'on-cloud' WTTS, $WTTS_2$ are 'off-cloud' WTTS. For P the subscripts G, L, and PP refer to the Gehan, logrank and Peto-Peto tests, respectively, while the superscripts A and M refer to the age and mass distributions.

Samples	P_G^A	P_L^A	P_{PP}^A
CTTS - $WTTS_1$	0.0046	0.0634	< 0.0001
$WTTS_1$ - $WTTS_2$	0.0002	0.0004	< 0.0001
CTTS - $WTTS_2$	< 0.0001	< 0.0001	< 0.0001
	P_G^M	P_L^M	P_{PP}^M
CTTS - $WTTS_1$	< 0.0001	< 0.0001	< 0.0001
$WTTS_1$ - $WTTS_2$	0.0002	0.0027	< 0.0001
CTTS - $WTTS_2$	< 0.0001	< 0.0001	< 0.0001

7. Spatial distribution and age

In Fig. 4 we plot the spatial distribution of TTS in Lupus, with stars in three different (arbitrary chosen) age bins ($\log(age/yrs) < 6.7, 6.7 \leq \log(age/yrs) <$

Fig. 4. Plot of the spatial distribution of TTS in Lupus. Right panel: optically selected TTS known prior to ROSAT, left panel: X-ray selected TTS discovered by ROSAT. Stars younger than $\log{(age/yrs)} = 6.7$ are denoted by filled squares, stars in the range $6.7 \le \log{(age/yrs)} < 7.0$ by open squares, and stars older than $\log{(age/yrs)} = 7.0$ by starred symbols. Also plotted are the two lowest contours of the CO map of Murphy et al. (1986). Note that the CO map covers only part of the area where TTS have been found.

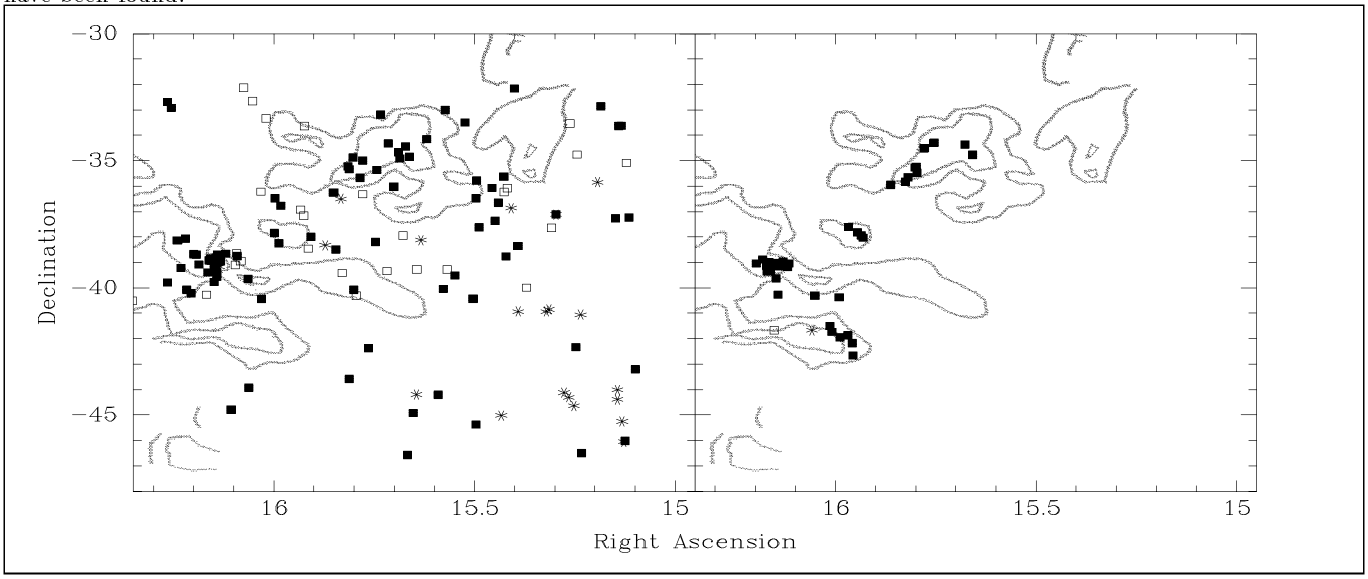

$7.0, \log{(age/yrs)} \ge 7.0$) coded by different symbols. Evidently, although many of the stars found at large distances from the clouds are comparatively old, there seems to be a significant fraction of stars which are younger than 5×10^6 yrs, yet located at distances of up to 10^o from the Lupus dark clouds (which are marked by the optically selected TTS). If these stars have been formed in the vicinity of the dark clouds, a velocity of at least 5 km/s is required for them to reach their present location, thus implying a velocity dispersion of $\ge 5/\sqrt{3} \approx 3$ km/s. This value is in excess of typical velocity dispersions of $\approx 1 - 2$ km/s, as found in SFRs like Taurus-Auriga (Jones & Herbig 1979) and Chamaeleon (Dubath et al. 1995). A possible explanation might be dynamical interactions in multiple TTS systems, producing run-away stars with high velocities (Sterzik et al. 1995, Sterzik & Durisen 1995). Also in-situ formation in small cloudlets, which have dispersed by now, has been suggested (Feigelson 1996). Young stars at quite large distances from dark clouds have also been found south of the Taurus-Auriga SFR (Neuhäuser et al. 1995b).

8. Correlations between X-ray emission and other stellar properties

In order to investigate the X-ray emission of TTS more closely, we studied correlations between the X-ray emission and other stellar properties of the stars of our sample. For completeness, data from Hughes et al. (1994) on the optically selected TTS in Lupus were incorporated. All X-ray data are taken from Krautter et al. (1996).

We determined Hα-luminosities $L_{H\alpha}$ by scaling the Hα-equivalent width with the stellar luminosity in the R_C band. In order to obtain the chromospheric fluxes, we corrected $L_{H\alpha}$ individually for the photospheric absorption by adding the mean Hα absorption of a main-sequence star of the respective spectral type to the measured equivalent width of our WTTS. This correction was determined from spectral standard stars observed during the runs for the optical identification of our new WTTS (Krautter et al. 1996). The results are plotted in Fig. 5. It can be seen that the RASS-selected 'off-cloud' WTTS show high X-ray surface fluxes F_X independent of the Hα surface flux $F_{H\alpha}$, while 'on-cloud' WTTS as well as CTTS exhibit a large spread of F_X for any given $F_{H\alpha}$, with the CTTS sytematically displaced towards higher $F_{H\alpha}$. For our sample of Lupus TTS, we observe a strong anticorrelation of $L_{H\alpha}$ vs. L_X only, if all TTS are taken into account, while no correlation is found within either one of the three subsets defined above (see Table 5). As the Hα luminosity of CTTS, contrary to that of WTTS, contains a large non-chromospheric contribution from the accretion disk and the stellar wind, while their mean X-ray luminosity is significantly lower than that of WTTS, we conclude that the observed anticorrelation within the whole sample reflects different sources responsible for the Hα emission of CTTS and WTTS rather than a physical (anti-)correlation between $L_{H\alpha}$ and L_X. In a study of the X-ray emission of TTS in Taurus-Auriga, Neuhäuser et al. (1995a) also could not find a correlation of $H\alpha$ emission and L_X.

If we examine the correlation of the equivalent width $W_{H\alpha}$ vs. L_X rather than $L_{H\alpha}$ vs. L_X, the increase of pho-

Fig. 5. Plot of X-ray surface flux F_X vs. Hα surface flux $F_{H\alpha}$. CTTS are denoted by filled circles, 'on-cloud' WTTS by open circles and 'off-cloud' WTTS by starred symbols. Arrows represent CTTS with upper limits on F_X.

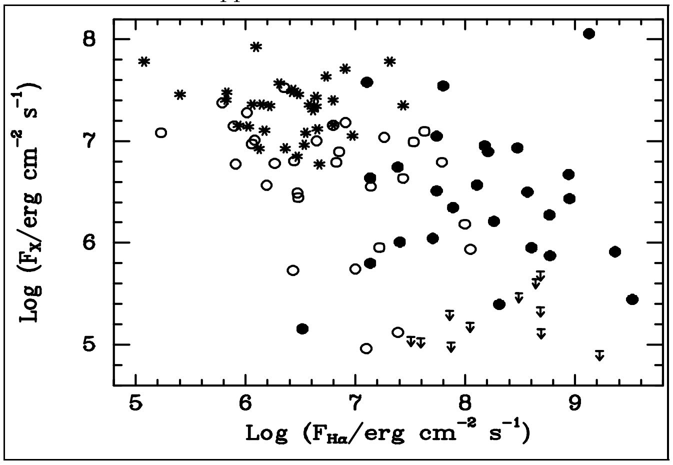

tospheric absorption and continuum flux for early spectral type, which causes a decrease of $W_{H\alpha}$, can produce correlations with the X-ray emission, especially for the 'on-cloud' WTTS, which span a large range of spectral types, as can be seen from Table 5.

For active late-type main-sequence stars Fleming et al. (1989) found an upper limit to the surface X-ray flux F_X, such that the maximum L_X for a given stellar radius $R_\star$ scales as $R_\star^2$. Thus, for a sample of X-ray selected TTS, which preferentially contains X-ray bright stars, a correlation of L_X with $R_\star$ is expected, if the X-ray emission mechanism of TTS is the same as for late-type dwarfs, while for the surface flux F_X no correlation with $R_\star$ should be observed. These effects can be observed for our sample of RASS-detected 'off-cloud' WTTS.

It is usually assumed that the X-ray emission of TTS and other late-type stars is caused by magnetic heating of the corona (cf. Montmerle & André 1988, Montmerle 1990). In this model, saturation is expected to occur when the stellar surface is completely covered by active regions, and therefore X-ray bright stars at the saturation limit show a constant F_X. Fleming et al. (1989) have found a value of $\sim 7 \times 10^7\,\mathrm{erg\,sec^{-1}\,cm^2}$ for this saturation limit.

For CTTS, most of which are well below this saturation limit (see Fig. 7), thus F_X can increase during the contraction.

In recent studies of TTS X-ray emission a correlation of L_X with the bolometric luminosity $L_\star$ has been observed (cf. Neuhäuser et al. 1995a, Feigelson et al. 1993, Strom & Strom 1994, Casanova et al. 1995). This observation is complicated by the fact that the slope of the observed $\log(L_X) \propto a \log(L_\star)$ relation is different in different SFR. While Strom & Strom (1994) infer $a = 1.80$ from their deep ROSAT pointed observation centered on V410 Tau, Neuhäuser et al. (1995a) find $a = 1.08$ for Taurus-Auriga, in agreement with Feigelson et al. (1993) and Casanova et al. (1995), who evaluated deep ROSAT pointed observations in Chamaeleon and ρ Oph, respectively.

In Fig. 6 we plot $\log(L_X)$ vs. $\log(L_\star)$ for Lupus TTS. Using statistical tests (see Table 5), we conclude that a correlation of $\log(L_X)$ with $\log(L_\star)$ is indeed present for both the 'off-cloud' WTTS and the 'on-cloud' WTTS, but not for the CTTS. Now, if all stars in a given sample had

Fig. 6. Plot of X-ray luminosity L_X vs. bolometric luminosity $L_\star$. CTTS are denoted by filled circles, 'on-cloud' WTTS by open circles and 'off-cloud' WTTS by starred symbols.

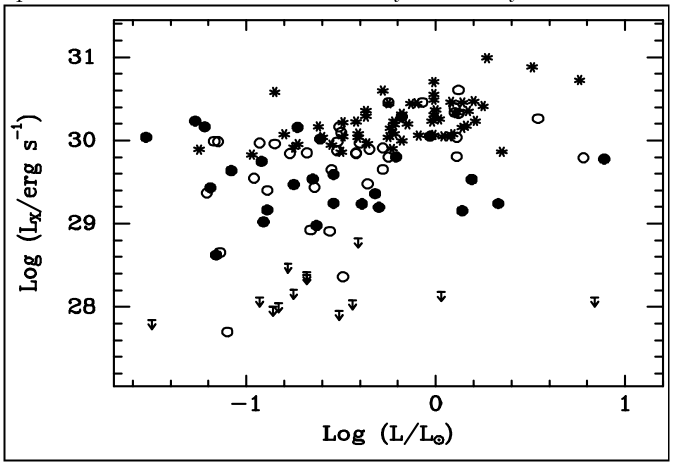

the same surface flux, and if within this sample there were some relation $R_\star \propto L_\star^b$, then we would expect $L_X \propto R_\star^2 \propto L_\star^{2b}$, i.e., $a \approx 2b$, which, within the errors, is consistent with our results for the RASS-discovered WTTS in Lupus (Table 5).

However, if F_X as well as $R_\star$ show some trend to increase with $L_\star$ (which might be due to selection effects, as will be discussed below), the situation is more complicated, and the combined effect of both will produce a stronger correlation of L_X with $L_\star$ rather than with $R_\star$.

As the magnetic activity of T Taur stars presumably is caused by a dynamo process, some correlation between L_X and stellar rotation is expected. Such a correlation has in fact been observed (cf. Bouvier & Bertout 1989, Neuhäuser et al. 1995a).

It has also been observed that on the approach to the main sequence, the rotational velocities of young stars first increase (cf. Bouvier et al. 1993, Edwards et al. 1993), and then decrease again, as discussed in Soderblom et al. (1993). This observation is explained in the framework of a model which suggests that during the CTTS phase the star is magnetically coupled to its disk, thus preventing a spin-up during contraction (Camenzind 1990, Cameron & Campbell 1993). After the dissipation of the disk, the star can spin up due to contraction and angular momentum conservation, while later on magnetic braking caused by the interaction of stellar magnetic field and stellar wind occurs. (cf. MacGregor & Brenner 1991, Bouvier & Forestini 1995). If X-ray activity in fact depends upon rotation, we expect it to rise with age first, and then fall again among young stars, like the rotational velocities. For young clusters it is known that the mean X-ray luminosity of their stars decreases with the age of the cluster (Stauffer et al. 1994, Pye et al. 1994), while on the other hand for TTS the X-ray luminosity L_X increases significantly from CTTS to WTTS, as expected from this model (see Table 5). Moreover, the CTTS in Lupus show an anticorrelation of F_X and $R_\star$ rather than a correlation of L_X and $R_\star$, which might indicate that for these stars L_X rather than F_X is about constant with radius, in line with the idea of disk-locking of the rotation.

Fig. 7. Plot of X-ray surface flux F_X vs. age. CTTS are denoted by filled circles, 'on-cloud' WTTS by open circles and 'off-cloud' WTTS by starred symbols.

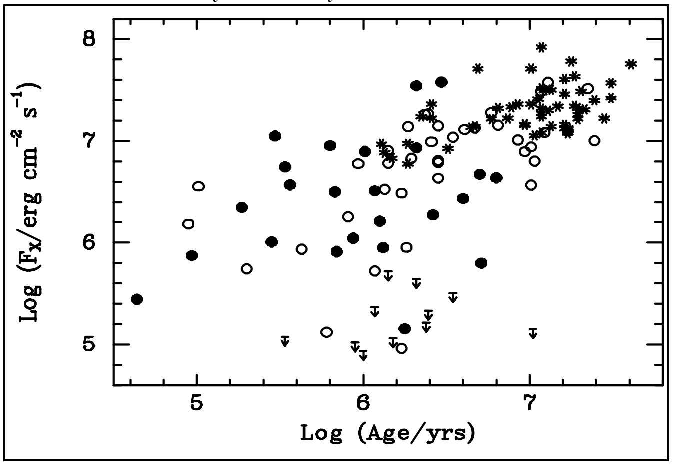

Fig. 8. Plot of X-ray surface flux F_X vs. stellar mass $M_\star$. CTTS are denoted by filled circles, 'on-cloud' WTTS by open circles and 'off-cloud' WTTS by starred symbols.

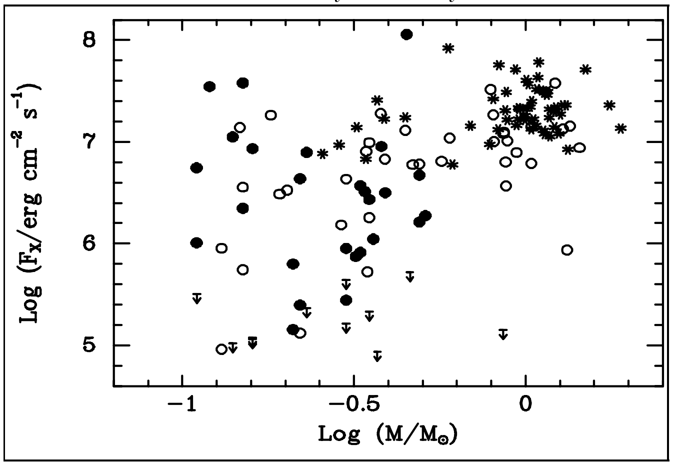

In Fig. 7, we plot the X-ray surface flux F_X vs. stellar age for the Lupus TTS. It can be seen that the maximum X-ray surface flux increases with age, with none of the youngest stars displaying comparatively high values of F_X. Statistical tests (see Table 5) give evidence of a correlation of F_X with age for the WTTS, while no correlation shows up for the CTTS. However, this might be due to the large scatter of F_X for the CTTS, as Fig. 7 shows that even for the CTTS alone the *maximum* values of F_X increase with age. An increase of F_X with age has also been observed by Neuhäuser et al. (1995a) for Taurus-Auriga TTS.

As within our sample, due to selection effects, the oldest stars probably are also the most luminous, this might be the physical reason for the observed correlation of F_X with $L_\star$ (there seems to be no significant correlation of $L_\star$ and age, probably due to the large scatter, but the mean values of $\log(age/yrs)$ of CTTS, 'on-cloud' WTTS and 'off-cloud' WTTS are 6.0, 6.4 and 7.0, respectively, while the mean luminosities $\log(L_\star/L_\odot)$ are -0.56, -0.45 and -0.21). Thus, within our sample there seems to be at least some trend for $L_\star$ to increase with age.

Fig. 8 shows the X-ray surface flux F_X vs. stellar mass $M_\star$ in our sample. It can be seen that nearly all of the 'off-cloud' WTTS have relatively high masses as well as strong X-ray emission, which presumably reflects the selection effect due to the flux limit of the RASS. On the other hand, for the optically selected CTTS there is a large spread of F_X at any given mass. No correlation between mass and F_X is observed for both samples.

'On-cloud' WTTS show the same large spread of F_X as the CTTS at low masses. At high masses, only WTTS with high F_X are detected. However, this might be explained by the fact that the 'on-cloud' WTTS with highest mass are also the oldest within this sample.

The Lupus CTTS are unbiased with respect to L_X and consist of younger and less massive stars than the WTTS. The 'on-cloud' WTTS, which have been discovered by pointed ROSAT observations, are much less biased towards stars with large L_X than the 'off-cloud' WTTS. Also on average they are younger, in line with their location near the dark clouds. The discussion above has shown the importance of both selection and evolutionary effects, which can explain the observed difference between these three subsamples with respect to the correlations in Table 5.

9. Hardness Ratios

The X-ray hardness ratios HR1 and HR2 are defined as

$$\mathrm{HR\,1} = \frac{C_B - C_A}{C_B + C_A} \quad \text{and} \quad \mathrm{HR\,2} = \frac{C_D - C_C}{C_D + C_C}, \tag{1}$$

where C_A, C_B, C_C, and C_D denote the count rates in the energy bands 0.1 to 0.4 keV, 0.5 to 2.1 keV, 0.5 to 0.9 keV and 0.9 to 2.1 keV, respectively. As can be seen from Table 4, for our three samples of Lupus TTS (CTTS, 'on-cloud' WTTS, and 'off-cloud' WTTS) obviously the mean values of HR1 and HR2 decrease in the same order as the mean extinction for these sample, i.e. the CTTS have the hardest X-ray emission and the highest extinction, while the 'off-cloud' WTTS have the softest X-ray emission as well as the lowest extinction. In Fig. 9 we show HR1 (lower panel) as well as the error in HR1 (upper panel) as function of L_X for Lupus WTTS. It seems that most of the scatter in HR1 is caused by errors rather than by an intrinsic scatter in HR1, as both the errors in HR1 and the observed scatter are of comparable magnitude. For HR2 (not plotted) the situation is quite similar. These observations indicate that WTTS might have intrinsically soft X-ray spectra, and that harder spectra, i.e., higher values of the hardness ratio, are caused by absorption. We also presume, that the intrinsic spectral energy distribution of WTTS has a rather small scatter around some mean value, i.e. most of the observed spread in the hardness ratios is due to large errors for weak sources, as can be inferred from Fig. 9. This conclusion is not applicable to the CTTS in Lupus. These are generally strongly absorbed, weak X-ray sources with hard X-ray spectra, but large errors in HR. Thus, it is not clear whether their hard X-ray spectra are due solely to absorption, or whether they are intrinsically different to that of WTTS.

Table 4. Mean values of HR1, HR2 and $E_{(B-V)}$ for Lupus TTS. Also given are errors of the mean, i.e. (standard deviation)/$\sqrt{N}$.

Sample	N	HR1	HR2	$E_{(B-V)}$
CTTS	26	0.95±0.02	0.38±0.03	0.32±0.05
WTTS$_{on-cloud}$	33	0.54±0.07	0.15±0.04	0.17±0.03
WTTS$_{off-cloud}$	48	0.24±0.05	0.10±0.06	0.12±0.01

10. Conclusions

In this work, we have performed a photometric study of the population of Lupus WTTS recently discovered by Krautter et al. (1996).

One of our most important results is that the new WTTS represent an older population than the hitherto known CTTS in Lupus. This finding is in agreement with the spatial distribution of these stars: while the CTTS are located in the vicinity of the dark clouds, as one would expect for young stars, the newly found WTTS are spread over a large area of more than 200 square degrees. We presume that these WTTS also formed in the Lupus dark clouds, and have spread over a large region due to their velocity dispersion.

Fig. 9. Plot of X-ray hardness ratio HR1 vs. L_X (lower panel) and error in HR1 vs. L_X (upper panel). 'On-cloud' WTTS are denoted by open circles and 'off-cloud' WTTS by starred symbols. In the upper panel the distinction between data from pointed observations and the RASS is clearly visible.

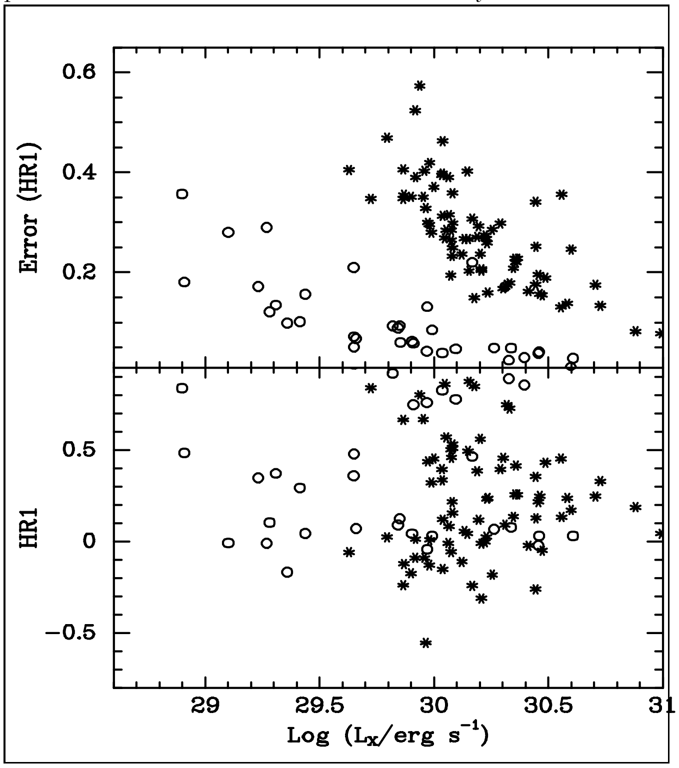

For most of the Lupus WTTS, a velocity dispersion of $1 - 2$ km/s as determined by Jones & Herbig (1979) for Taurus-Auriga and by Dubath et al. (1995) for Chamaeleon would be sufficient to explain their spatial distribution, given the ages determined by us. However, some WTTS, which are relatively young, but are located at large distances to the dark clouds, might also be ejected with high velocities by three-body interactions in the way proposed by Sterzik & Durison (1995).

Furthermore, comparing the masses of the newly found WTTS in Lupus with those of the CTTS, there seems to be some evidence that the IMF of the CTTS, (i.e. the youngest TTS in Lupus), shows some deficit at high masses with respect to the (older) WTTS. Thus possibly, the IMF has become steeper during the history of the Lupus SFR. A deficit of young high-mass TTS like that observed for the Lupus SFR has not been found in other SFR's, but this might be due to the fact that the Lupus SFR is significantly older than other well-studied SFR's (Hughes et al. 1994).

Our study of the correlations between the X-ray emission of Lupus TTS and other stellar parameters indicates that the X-ray emission of TTS is similar to that of other active late-type stars, and possibly is caused by the same mechanism, i.e. coronal heating by magnetic activity caused by a dynamo mechanism. Obviously, the X-ray emission of TTS is limited by the same saturation limit than that one of other active late-type stars. Moreover, we can show that the X-ray surface flux increases with stellar age. An increase with stellar age has also been observed for the rotational velocities of TTS (cf. Bouvier et al. 1993, Edwards et al. 1993). Thus, the observed increase of the X-ray surface flux with age is in qualitative agreement with the idea that the magnetic activity in TTS is correlated with rotation via a dynamo mechanism. We do not have direct evidence for such a correlation, because only few measurements of the rotational velocities of Lupus TTS have been done yet, but for Taurus TTS such a correlation has indeed been found (cf. Bouvier 1990, Neuhäuser et al. 1995a).

As stellar parameters like bolometric luminosity, radius, mass, and (in the special case of our sample) also age correlate with each other, it is difficult to determine which parameters are the most important for the X-ray emission. In current theories, which link the X-ray emission to coronal heating caused by magnetic activity, basic parameters are the stellar rotation (which enters in our data via age and stellar rotational evolution), and, for stars near the saturation limit for F_X, the stellar surface area (which enters via the radius). From our analysis we cannot rule out possible additional parameters. However, it seems that, if the evolution of stellar rotation is taken into account, our observations can be explained without the introduction of additional parameters.

Acknowledgements. This research was supported by grant KR 1053/3 from the DFG, Germany, grant 50OR90017 (Verbundforschung Astronomie) from the BMFT, Germany, and from CONACyT, Mexico. The ROSAT project is supported by the Bundesministerium für Bildung, Wissenschaft, Forschung und Technologie (BMBF/DARA) and the Max-Planck-Gesellschaft. This research has made use of the SIMBAD database, operated at CDS, Strasbourg, France.

References

Alcalá J.M., Krautter J., Schmitt J.H.M.M. et al. 1996a, A&A, in press
Alcalá J.M., Krautter J., Covino E. et al. 1996b, A&A, submitted
Alexander D.R., Augason G.C., Johnson H. R. 1991, ApJ 345, 1014
Barnes T.G., Evans D.S. 1976, MNRAS 174, 489
Bessel M. S. & Brett J. M. 1988, PASP 100, 1134
Bessel M. S. 1991, AJ 101, 662
Bouchet P., Schmider F.X., Manfroid J. 1991, A&ASS 91, 409
Bouvier J., Bertout C. 1989, A&A 211, 99
Bouvier J. 1990, AJ 99, 946
Bouvier J., Forestini M. 1995, in: Circumstellar Dust Disks and Planet Formation, ed. R. Ferlet, in press
Bouvier J., Cabrit C., Fernandez M., Martín E.L., Mathews J. 1993a, A&A 272, 176
Brandner W., Alcalá J.M., Kunkel M., Moneti A., Zinnecker H. 1996, A&A 307, 121
Casanova S., Montmerle T., Feigelson E.D., Andre P. 1995, ApJ 439, 752
Camenzind M. 1990, Rev. Mod. Astron. 3, ed. G. Klare, Heidelberg, Springer press, p. 234
Cameron A.C., Campbell C.G. 1993, A&A 274, 309
Covino E., Terranegra L., Franchini M., Chavarria-K. C., Stalio R. 1992, A&AS 94, 273
D'Antona F., Mazzitelli I. 1994, ApJSS 90, 467
Dubath P., Reipurth B., Mayor M. 1995, ESO scientific preprint, No. 1108
Edwards S, Strom S.E., Hartigan P. et al. 1993, AJ 106, 372
Feigelson E.D., Casanova S., Montmerle T., Guibert J. 1993, ApJ 416, 623
Feigelson E.D., 1996, ApJ, in press
Fleming, T. A., Gioia, I. M., Maccacaro, T. 1989, ApJ 340, 1011
Ghez, A.M., Neugebauer, G., Matthews, K. 1993, AJ 106, 2005
Graham, J.A. 1982, PASP 94, 244
Hartigan P., Kenyon S.J., Hartmann L. et al. 1991, ApJ 382, 617
Herbig, G.H. 1978, in Problems of Physics and Evolution of the Universe, Erevan, Acad. Sci. Armen. SSR
Hughes, J., Hartigan, P., Clampitt, L. 1993, AJ 104, 680
Hughes, J., Hartigan, Krautter, J., Kelemen, J. 1994, AJ 108, 1071
Jones B.F., Herbig G.H. 1979, AJ 84, 1872
Krautter, J. 1991, in Low Mass Star Formation in Southern Molecular Clouds, ESO Report No. 11, edt. B. Reipurth, p. 127
Krautter J., Wichmann, R., Schmitt et al. 1996, AA in press
Lacy C.H. 1977, ApJSS 34, 479
Leinert, C., Zinnecker, H., Weitzel, N. et al. 1993, AA 278, 129
MacGregor K.B., Brenner M. 1991, ApJ 376, 204
Montmerle, T., André 1988, in Formation and Evolution of Low Mass Stars, eds. A.K. Dupree, M.T.V.T. Lago, p. 127
Montmerle, T. 1990, Rev. Mod. Astron. 3, edt. G. Klare, Heidelberg, Springer, p. 209
Murphy D.C., Cohen R., May J. 1986, A&A 167, 234
Neuhäuser, R., Sterzik, M.F., Schmitt, J.H.M.M., Wichmann, R. Krautter, J. 1995a, A&A 297, 391
Neuhäuser, R., Sterzik, M.F., Torres, G., Martin, E.L. 1995b, A&A 299, L13
Pye J.P., Hodgkin S.T., Stern R.A., Stauffer J.R. 1994, MNRAS 266, 798
Reipurth B., Zinnecker H. 1993, A&A 278, 81
Schmidt-Kaler T. H. 1982, Physical Parameters of Stars, Landolt-Bornstein New Series Vol. 2b, eds. K. Schaifers & H.H.Voigt, Springer
Schwartz, R. D. 1977, ApJSS 35, 161
Soderblom D.R., Stauffer J.R., MacGregor K.B., Jones B.F. 1993, ApJ 409, 624
Stauffer J.R., Caillault J.-P., Gagne M., Prosser C.F., Hartmann L.W. 1994, ApJS 91, 625
Sterzik M.F., Alcalá J.M., Neuhäuser R., Schmitt J.H.M.M. 1995, A&A 297, 418
Sterzik M.F., Durisen R.H. 1995, A&A 304, L9
Strom K.M., Strom S.E. 1994, ApJ 424, 237
Wichmann, R., Krautter, J., Schmitt, J.H.M.M. et al. 1996, A&A 312, 439

Table 6. Photometry of Lupus T Tauri stars. For JHKL individual errors in hundredths of magnitude are given in brackets.

Designation	V	B-V	U-B	V-R_C	V-I_C	J	H	K	L
RXJ1505.9-4311	12.58	1.35	1.25	0.83	1.63	9.91 (1)	9.23 (2)	9.03 (2)	
RXJ1506.9-3714	13.38	1.16	1.01	0.65	1.26	11.30 (3)	10.57 (2)	10.43 (2)	
RXJ1507.2-3505	10.53	0.88	0.43	0.51	0.96	9.03 (1)	8.48 (1)	8.34 (1)	8.13 (15)
RXJ1507.6-4603	11.64	0.97	0.60	0.57	1.12				
RXJ1507.9-4515	10.81	0.68	0.11	0.43	0.83				
RXJ1508.6-4423	10.63	0.69	0.14	0.41	0.80	9.36 (1)	8.91 (1)	8.78 (1)	8.71 (35)
RXJ1508.7-4400	10.39	0.71	0.16	0.42	0.83	9.03 (1)	8.55 (1)	8.43 (1)	8.41 (26)
RXJ1511.1-3251	11.92	1.23	1.01	0.76	1.48				
RXJ1511.6-3550	12.59	1.10	0.91	0.68	1.38				
RXJ1514.0-4629A	14.35	1.49	0.70	1.02	2.20				
RXJ1514.0-4629B	12.72	1.27	1.24	0.83	1.55				
RXJ1514.2-4103	10.38	0.61	0.04	0.36	0.74				
RXJ1514.7-3445	9.63	0.30	-0.06	0.30	0.61				
RXJ1514.8-4220	13.85	0.91	0.44	0.48	0.89	12.34 (5)	11.90 (5)	11.68 (7)	
RXJ1515.1-4438	13.64	1.43	1.28	0.92	1.80				
RXJ1515.8-3331	10.69	0.88	0.43	0.52	1.00	9.05 (1)	8.50 (1)	8.38 (1)	7.95 (10)
RXJ1515.9-4418	12.68	1.11	0.85	0.65	1.35				
RXJ1516.6-4406	11.93	1.04	0.75	0.64	1.20				
RXJ1517.8-3706A	13.91	1.40	1.34	1.01	2.11				
RXJ1517.8-3706B	14.82	1.43	0.80	0.91	2.07				
RXJ1518.5-3738	10.92	0.87	0.44	0.51	1.01	9.20 (1)	8.66 (1)	8.52 (1)	8.26 (16)
RXJ1518.9-4050	11.01	0.91	0.48	0.53	1.04	9.25 (1)	8.70 (1)	8.56 (1)	8.68 (54)
RXJ1519.3-4056						9.46 (2)	8.91 (1)	8.75 (1)	
RXJ1522.2-3959	12.02	1.07	0.77	0.65	1.29	9.83 (1)	9.23 (1)	9.06 (1)	
RXJ1523.4-4055	11.87	1.03	0.70	0.63	1.16				
RXJ1523.5-3821	14.15	1.68	0.72	0.99	2.38				
RXJ1524.0-3209	12.38	1.25	1.06	0.82	1.73				
RXJ1524.5-3652	11.30	0.91	0.48	0.52	1.01				
RXJ1525.1-3604	10.92	0.96	0.55	0.57	1.09				
RXJ1525.3-3845	8.75	0.67	0.14	0.40	0.76				
RXJ1525.5-3613	11.59	0.98	0.60	0.62	1.21				
RXJ1525.6-3537	12.44	1.24	0.93	0.80	1.59				
RXJ1526.0-4501	10.87	0.79	0.31	0.45	0.87	9.45 (2)	9.01 (1)	8.90 (1)	8.39 (20)
RXJ1526.9-3721	13.02	1.40	1.05	0.89	1.85				
RXJ1529.3-3737	13.72	1.52	1.04	0.99	2.36				
RXJ1533.0-3930	13.10	1.51	1.32	0.96	1.98				
RXJ1534.1-3916	10.79	0.84	0.38	0.49	0.95				
RXJ1534.6-4002	11.98	1.23	1.03	0.76	1.45	9.55 (1)	8.91 (1)	8.76 (1)	8.78 (44)
RXJ1538.0-3807	12.39	1.15	1.00	0.71	1.36				
RXJ1538.6-3916	11.47	1.01	0.72	0.59	1.13				
RXJ1538.7-4411	10.56	0.85	0.36	0.49	0.98				
RXJ1540.7-3756	12.35	1.19	1.05	0.74	1.42				
RXJ1543.1-3920	12.25	1.19	1.02	0.74	1.42				
RXJ1545.9-4222	10.59	0.99	0.63	0.59	1.15	8.64 (1)	8.05 (1)	7.90 (1)	7.70 (14)
RXJ1546.7-3618	11.28	0.89	0.41	0.53	1.07	9.40 (1)	8.88 (1)	8.74 (1)	
RXJ1547.7-4018	11.08	0.95	0.61	0.55	1.05	9.36 (1)	8.82 (1)	8.68 (1)	
RXJ1548.0-4004	12.50	1.30	1.08	0.82	1.75				
RXJ1548.1-3452	13.83	1.49	0.85	0.97	2.26				
RXJ1549.7-3925	10.55	0.92	0.51	0.53	1.03	8.78 (1)	8.26 (1)	8.13 (1)	9.16 (93)
RXJ1550.0-3629	11.52	0.98	0.63	0.57	1.11				
RXJ1550.8-3830	13.44	1.52	1.44	0.97	2.02	9.97 (2)	9.19 (1)	8.94 (1)	9.11 (38)

Table 6. Photometry of Lupus T Tauri stars

Designation	V	B-V	U-B	V-R_C	V-I_C	J	H	K	L
RXJ1552.3-3819	13.19	1.27	1.34	0.76	1.64	10.44 (2)	9.74 (2)	9.52 (2)	9.31 (68)
RXJ1554.9-3827	13.43	1.40	1.01	0.89	1.86				
RXJ1555.4-3338	12.45	1.13	0.93	0.71	1.40				
RXJ1555.6-3709	12.52	1.23	1.02	0.75	1.48				
RXJ1556.1-3655	13.85	1.20	-0.14	0.94	1.99	10.33 (2)	9.51 (1)	9.08 (2)	8.18 (18)
RXJ1559.0-3646	13.57	1.44	0.85	0.98	2.19				
RXJ1559.3-3814	13.62	1.40	1.41	0.96	2.15				
RXJ1559.8-3628	11.00	1.12	0.89	0.68	1.34				
RXJ1559.9-3750	13.03	1.57	1.24	0.80	2.06				
RXJ1601.2-3320	10.88	0.89	0.34	0.53	1.07	9.06 (1)	8.55 (1)	8.39 (1)	8.23 (23)
RXJ1602.0-3613	11.96	1.06	0.73	0.67	1.39	9.66 (1)	9.00 (1)	8.81 (1)	9.10 (32)
RXJ1603.2-3239	12.94	1.31	0.88	0.80	1.69				
RXJ1603.8-4355	9.67	0.92	0.50	0.53	1.02	8.00 (1)	7.46 (1)	7.31 (1)	7.25 (08)
RXJ1603.9-3938	11.02	1.05	0.76	0.64	1.23				
RXJ1604.5-3207	10.86	0.89	0.44	0.50	1.02				
RXJ1605.0-3857	9.36	0.47	-0.08	0.39	0.35	8.18 (1)	7.94 (1)	7.88 (1)	7.89 (14)
RXJ1605.5-3846	13.78	0.76	0.13	0.50	0.55	11.91 (6)	11.53 (4)	11.42 (9)	
RXJ1605.6-3837	14.38	1.46	0.69	0.90	1.29	10.82 (3)	10.10 (2)	9.89 (3)	
RXJ1605.8-3905	10.49	0.80	0.31	0.47	0.43				
RXJ1607.2-3839	12.76	1.35	1.11	0.89	0.92	9.73 (2)	9.02 (2)	8.81 (2)	8.42 (23)
RXJ1608.0-3857	12.77	1.43	0.96	0.91	1.00	9.68 (1)	8.94 (1)	8.73 (1)	8.69 (26)
RXJ1608.2-3910	12.84	1.24	1.07	0.78	0.68	10.46 (2)	9.81 (1)	9.64 (2)	
RXJ1608.3-3843	12.23	1.28	1.03	0.80	0.83	9.60 (3)	8.94 (1)	8.78 (2)	8.50 (31)
RXJ1608.5-3900A	14.57	2.12	1.61	1.03	1.34	10.88 (4)	10.09 (1)	9.81 (2)	
RXJ1608.5-3900B	15.05	1.48	0.87	0.89	1.55	11.09 (6)	10.34 (2)	10.04 (2)	
RXJ1608.5-3847	13.72	2.23	0.39	1.07	1.37	9.80 (2)	8.98 (1)	8.66 (1)	8.14 (16)
RXJ1608.6-3922	13.48	1.52	1.01	1.01	1.02	9.99 (1)	9.14 (1)	8.69 (1)	
RXJ1608.9-3945	15.33	3.35		1.07	1.69	10.90 (3)	10.18 (5)	9.88 (2)	
RXJ1608.9-3905	10.88	1.03	0.66	0.60	0.54	9.04 (1)	8.47 (1)	8.30 (1)	8.21 (17)
RXJ1609.4-3855	14.42	1.67	2.13	1.01	1.55	9.82 (3)	9.06 (2)	8.78 (3)	8.49 (23)
RXJ1609.5-3850	12.72	1.39	1.17	0.91	1.06	9.45 (2)	8.73 (2)	8.52 (2)	8.25 (19)
RXJ1609.7-3854	11.56	1.30	1.14	0.79	0.77	8.90 (1)	8.22 (1)	8.02 (1)	7.87 (12)
RXJ1609.9-3923	14.37	1.44	0.27	1.02	1.58	9.99 (3)	9.17 (1)	8.85 (1)	
RXJ1610.1-4016	11.20	0.97	0.59	0.56	0.53	9.40 (2)	8.85 (2)	8.70 (2)	8.29 (20)
RXJ1611.6-3841	13.40	1.91	1.74	1.12	1.06	11.14 (3)	10.46 (2)	10.25 (3)	
RXJ1612.0-3840	11.69	1.30	1.13	0.82	0.78	9.19 (3)	8.49 (1)	8.27 (1)	8.18 (22)
RXJ1613.0-4004	13.49	1.61	1.38	0.98	1.15	9.90 (1)	9.10 (1)	8.83 (1)	
RXJ1613.9-3912	15.43	1.56	2.24	0.94	1.80				
RXJ1615.3-3255	12.00	1.22	0.66	0.79	0.71				
RXJ1621.2-4030	10.45	0.82	0.37	0.49	0.40				
RXJ1623.5-3958	10.82	0.67	0.14	0.42	0.37				

This article was processed by the author using Springer-Verlag LaTeX A&A style file *L-AA* version 3.

Table 7. Stellar properties of Lupus T Tauri stars. Masses and ages are from evolutionary tracks by D'Antona and Mazzitelli (1994).

Designation	Spectral type	T_{eff} [K]	$\log(L_\star/L_\odot)$	A_V [mag]	$R_\star/R_\odot$	$M_\star/M_\odot$	log (age) [yr]	$\Delta(H-K)$ [mag]
J1506.9-3714	K0	5248.0	-0.70	0.94	0.54	0.80	>7.45	0.00
J1507.2-3505	K0	5248.0	0.14	0.20	1.43	1.32	6.89	0.05
J1507.6-4603	K2	4897.0	-0.22	0.35	1.09	1.04	7.11	
J1507.9-4515	G3	5715.0	0.04	0.35	1.07	1.05	7.37	
J1508.6-4423	G8	5309.0	0.00	0.00	1.18	1.13	7.15	0.06
J1508.7-4400	G7	5390.0	0.14	0.15	1.35	1.25	7.03	0.05
J1511.1-3251	K6	4255.0	-0.18	0.39	1.51	0.73	6.31	
J1511.6-3550	K5	4406.0	-0.49	0.39	0.97	0.89	7.15	
J1514.0-4629A	M2	3499.0	-0.97	0.15	0.89	0.29	6.57	
J1514.0-4629B	K7	4150.0	-0.50	0.25	1.09	0.81	6.87	
J1514.2-4103	G7	5390.0	0.07	0.00	1.25	1.18	7.11	
J1514.7-3445	F5	5554.0	0.35	0.00	1.61	1.38	6.95	
J1514.8-4220	K1	4989.0	-1.25	0.00	0.32	0.80	>7.45	0.14
J1515.1-4438	M0	3801.0	-0.85	0.00	0.87	0.58	7.03	
J1515.8-3331	K0	5248.0	0.11	0.30	1.38	1.28	6.93	0.06
J1515.9-4418	K1	4989.0	-0.37	1.04	0.87	0.88	7.43	
J1516.6-4406	K2	4897.0	-0.24	0.54	1.06	1.02	7.15	
J1517.8-3706A	K7-M0	3899.0	-0.55	1.18	1.16	0.61	6.61	
J1517.8-3706B	M1.5	3573.0	-1.25	0.07	0.62	0.34	7.11	
J1518.5-3738	K1	4989.0	0.00	0.20	1.33	1.22	6.87	0.05
J1518.9-4050	G8	5309.0	0.09	0.59	1.31	1.23	7.03	0.03
J1519.3-4056	K0	5248.0	0.00	0.67	1.20	1.15	7.09	0.04
J1522.2-3959	K3	4688.0	-0.25	0.57	1.14	1.04	6.97	0.03
J1523.4-4055	K2	4897.0	-0.25	0.44	1.04	1.01	7.17	
J1523.5-3821	M2	3499.0	-0.75	0.59	1.15	0.30	6.27	
J1524.0-3209	K7	4150.0	-0.22	0.69	1.50	0.65	6.25	
J1524.5-3652	K1	4989.0	-0.15	0.20	1.12	1.08	7.09	
J1525.1-3604	K1	4989.0	0.08	0.39	1.48	1.30	6.73	
J1525.3-3845	G5	5554.0	0.76	0.07	2.60	2.06	6.45	
J1525.5-3613	K2	4897.0	-0.10	0.57	1.24	1.14	6.93	
J1525.6-3537	K6	4255.0	-0.28	0.67	1.34	0.80	6.53	
J1526.0-4501	G5	5554.0	0.02	0.35	1.11	1.05	7.31	0.03
J1526.9-3721	M0.5	3724.0	-0.60	0.00	1.21	0.46	6.39	
J1529.3-3737	M3	3349.0	-0.73	0.00	1.29	0.22	6.11	
J1533.0-3930	M1	3648.0	-0.55	0.10	1.33	0.40	6.64	
J1534.1-3916	K1	4989.0	-0.01	0.05	1.33	1.22	6.87	
J1534.6-4002	K6	4255.0	-0.22	0.32	1.42	0.76	6.41	0.01
J1538.0-3807	K5	4406.0	-0.42	0.35	1.06	0.92	7.01	
J1538.6-3916	K4	4592.0	-0.23	0.00	1.21	1.03	6.85	
J1538.7-4411	G5	5554.0	0.25	0.62	1.45	1.30	7.03	
J1540.7-3756	K6	4255.0	-0.41	0.25	1.16	0.86	6.81	
J1543.1-3920	K6	4255.0	-0.37	0.25	1.21	0.84	6.71	
J1545.9-4222	K1	4989.0	0.27	0.54	1.84	1.41	6.45	0.04
J1546.7-3618	K1	4989.0	-0.09	0.35	1.21	1.14	6.99	0.04
J1547.7-4018	K1	4989.0	-0.02	0.30	1.31	1.21	6.89	
J1548.0-4004	K7-M0	3899.0	-0.36	0.30	1.45	0.50	6.17	
J1548.1-3452	M2.5	3403.0	-0.80	0.00	1.15	0.25	6.21	
J1549.7-3925	K0	5248.0	0.20	0.37	1.52	1.38	6.83	0.03
J1550.0-3629	K2	4897.0	-0.18	0.32	1.14	1.08	7.03	
J1550.8-3830	K7	4150.0	-0.35	1.40	1.30	0.73	6.53	0.03
J1552.3-3819	K7	4150.0	-0.64	0.47	0.92	0.81	7.17	0.06
J1554.9-3827	K7	4150.0	-0.51	1.01	1.08	0.82	6.89	

Table 7. cont.

Designation	Spectral type	T_{eff} [K]	$\log(L_\star/L_\odot)$	A_V [mag]	$R_\star/R_\odot$	$M_\star/M_\odot$	log (age) [yr]	$\Delta(H-K)$ [mag]
J1555.4-3338	K5	4406.0	-0.41	0.44	1.07	0.93	6.99	
J1555.6-3709	K6	4255.0	-0.42	0.39	1.14	0.86	6.83	
J1556.1-3655	M1	3648.0	-0.87	0.07	0.93	0.42	6.73	0.23
J1559.0-3646	M1.5	3573.0	-0.62	0.37	1.28	0.35	6.19	
J1559.3-3814	M1.5	3573.0	-0.68	0.27	1.19	0.36	6.29	
J1559.8-3628	K3	4688.0	0.21	0.69	1.94	1.01	6.15	
J1559.9-3750	M0.5	3724.0	-0.50	0.42	1.36	0.44	6.21	
J1601.2-3320	G8	5309.0	0.16	0.67	1.43	1.32	6.93	0.06
J1602.0-3613	K3	4688.0	-0.13	0.81	1.30	1.09	6.77	0.04
J1603.2-3239	K7	4150.0	-0.49	0.59	1.11	0.81	6.85	
J1603.8-4355	K1	4989.0	0.51	0.22	2.42	1.45	6.11	0.06
J1603.9-3938	K3	4688.0	0.10	0.42	1.70	1.06	6.35	
J1604.5-3207	K2	4897.0	-0.01	0.10	1.37	1.21	6.79	
J1605.0-3857	G2	5794.0	0.54	0.15	1.85	1.43	6.97	0.00
J1605.5-3846	K2	4897.0	-1.16	0.17	0.37	0.80	>7.45	0.00
J1605.6-3837	M1	3648.0	-0.93	0.57	0.86	0.41	6.83	-0.03
J1605.8-3905	G9	5250.0	0.12	0.15	1.40	1.31	6.91	
J1607.2-3839	K7	4150.0	-0.28	0.89	1.40	0.69	6.39	0.02
J1608.0-3857	M0	3801.0	-0.42	0.27	1.43	0.46	6.15	0.02
J1608.2-3910	K6	4255.0	-0.55	0.35	0.98	0.85	7.11	0.03
J1608.3-3843	K7	4150.0	-0.25	0.44	1.45	0.68	6.33	0.00
J1608.5-3900A	M1.5	3573.0	-0.85	0.81	0.98	0.35	6.55	0.03
J1608.5-3900B	M3.5	3250.0	-1.25	0.00	0.74	0.16	6.37	0.03
J1608.5-3847	M2	3499.0	-0.50	0.74	1.53	0.30	5.90	0.06
J1608.6-3922	K6	4255.0	-0.25	1.75	1.38	0.78	6.47	0.22
J1608.9-3945	M3.5	3250.0	-1.21	0.30	0.79	0.16	6.43	0.01
J1608.9-3905	K2	4897.0	0.12	0.39	1.59	1.28	6.57	0.06
J1609.4-3855	M3.5	3250.0	-0.96	0.00	1.04	0.17	6.23	0.01
J1609.5-3850	M0.5	3724.0	-0.40	0.20	1.51	0.41	6.03	0.00
J1609.7-3854	K5	4406.0	0.11	0.84	1.95	0.73	5.97	0.04
J1609.9-3923	M1.5	3573.0	-0.59	1.38	1.33	0.35	6.15	0.03
J1610.1-4016	K2	4897.0	-0.07	0.27	1.29	1.17	6.87	0.04
J1611.6-3841	M2	3499.0	-0.56	0.10	1.42	0.30	6.03	0.00
J1612.0-3840	K5	4406.0	0.10	0.94	1.93	0.73	5.97	0.05
J1613.0-4004	K7	4150.0	-0.28	1.68	1.41	0.69	6.37	0.03
J1613.9-3912	M4	3147.0	-1.27	0.00	0.71	0.13	6.33	
J1615.3-3255	K5	4406.0	-0.12	0.69	1.50	0.85	6.39	
J1621.2-4030	G8	5309.0	0.17	0.22	1.44	1.33	6.91	
J1623.5-3958	G3	5715.0	0.00	0.25	1.02	1.03	7.41	